Journal of Human Evolution 81 (2015) 29–40

Contents lists available at ScienceDirect

Journal of Human Evolution

journal homepage: www.elsevier.com/locate/jhevol

Encephalization and diversification of the cranial base in platyrrhine primates

Leandro Aristide [a], Sergio F. dos Reis [b], Alessandra C. Machado [c], Inaya Lima [c], Ricardo T. Lopes [c], S. Ivan Perez [a, *]

[a] Division Antropologia, Facultad de Ciencias Naturales y Museo, UNLP, CONICET, 122 y 60, La Plata, Argentina
[b] Departamento de Biologia Animal, UNICAMP, Campinas, São Paulo, Brazil
[c] Laboratório de Instrumentação Nuclear, Centro de Tecnologia, UFRJ, Ilha do Fundão, Rio de Janeiro, Brazil

ARTICLE INFO

Article history:
Received 15 July 2014
Accepted 3 February 2015
Available online 2 March 2015

Keywords:
High resolution computed tomography
Geometric morphometrics
Phylogenetic comparative method
Phylogenetic structure
Basicranial flexion
Evolutionary modularity

ABSTRACT

The cranial base, composed of the midline and lateral basicranium, is a structurally important region of the skull associated with several key traits, which has been extensively studied in anthropology and primatology. In particular, most studies have focused on the association between midline cranial base flexion and relative brain size, or encephalization. However, variation in lateral basicranial morphology has been studied less thoroughly. Platyrrhines are a group of primates that experienced a major evolutionary radiation accompanied by extensive morphological diversification in Central and South America over a large temporal scale. Previous studies have also suggested that they underwent several evolutionarily independent processes of encephalization. Given these characteristics, platyrrhines present an excellent opportunity to study, on a large phylogenetic scale, the morphological correlates of primate diversification in brain size. In this study we explore the pattern of variation in basicranial morphology and its relationship with phylogenetic branching and with encephalization in platyrrhines. We quantify variation in the 3D shape of the midline and lateral basicranium and endocranial volumes in a large sample of platyrrhine species, employing high-resolution CT-scans and geometric morphometric techniques. We investigate the relationship between basicranial shape and encephalization using phylogenetic regression methods and calculate a measure of phylogenetic signal in the datasets. The results showed that phylogenetic structure is the most important dimension for understanding platyrrhine cranial base diversification; only *Aotus* species do not show concordance with our molecular phylogeny. Encephalization was only correlated with midline basicranial flexion, and species that exhibit convergence in their relative brain size do not display convergence in lateral basicranial shape. The evolution of basicranial variation in primates is probably more complex than previously believed, and understanding it will require further studies exploring the complex interactions between encephalization, brain shape, cranial base morphology, and ecological dimensions acting along the species divergence process.

Introduction

The primate skull is a highly modular structure comprising the face, neurocranium, and basicranium (Cheverud, 1996; Lieberman et al., 2000; Sperber, 2001). Although these units vary relatively independently, they can change in a correlated way with other anatomical traits during development and evolution due to structural and functional factors (Cheverud, 1996; Hallgrímsson and Lieberman, 2008). The basicranium, or cranial base, is a structurally important region associated with several key traits, including the brain, inner ear, nasal fossa, and orbits, and is articulated with the vertebral column (Moss and Young, 1960; Ross and Ravosa, 1993; Lieberman et al., 2000). Due to these characteristics, the cranial base has been extensively studied in anthropology and primatology, and its variation related to changes in other cranial regions and organs (Moss, 1972; Ross and Ravosa, 1993; Bastir et al., 2010). In particular, most of these previous studies have focused on traits of the midline cranial base (an important aspect of basicranial

* Corresponding author.
E-mail address: ivanperezmorea@gmail.com (S.I. Perez).

http://dx.doi.org/10.1016/j.jhevol.2015.02.003
0047-2484/

morphology; Ross and Ravosa, 1993; Lieberman et al., 2000; Bookstein et al., 2003; Bastir et al., 2010; Bruner et al., 2010), linking its degree of dorsoventral flexion (i.e., basicranial angle) to skull differences in face size and orientation, brain volume, and orbital orientation (e.g., Ross and Ravosa, 1993; Lieberman et al., 2000; Bastir et al., 2010).

Encephalization, or relative brain size, has largely been hypothesized to be the main factor influencing the evolution of the cranial base angle among primates (Moss and Young, 1960; Lieberman et al., 2008). Although many definitions of encephalization coexist, most recent works have linked basicranial flexion to brain volume relative to cranial base length (a measure of basicranial size; Ross and Ravosa, 1993; Lieberman et al., 2008). One of the most frequent explanations for this relationship in primates holds that a more flexed basicranium would generate more space for an enlarged brain to fit the braincase (the "spatial-packing" hypothesis; Biegert, 1957, 1963; Gould, 1977; Ross and Ravosa, 1993). In this sense, alternative definitions of encephalization lead to different versions of this hypothesis (Lieberman et al., 2008). Moreover, this association has been observed even in experimental models of mice (that have a considerably different cranial morphology compared to primates, with small brains and elongated faces; Lieberman et al., 2008), which highlights the likely ubiquity of the relationship between cranial base angle and relative brain size among mammals. If relative brain size is the main factor influencing basicranial morphology at different phylogenetic scales, similarity among species may occur due to changes in relative brain size, even when these changes occur in clades with different ancestral trait values (i.e., phenotypic convergence; Moen et al., 2013). Moreover, the signature of the branching process of the species during evolution on the observed pattern of morphological variation may also be an important factor in understanding its origins (Felsenstein, 1985), as has been suggested for the basicranial morphology of hominoid primates (Lockwood et al., 2004).

Past studies have also suggested that the basicranium is not a homogeneous morphological unit and that the midline cranial base, linked to the attachment of the brain, would constitute an ontogenetic and evolutionarily separate module from the lateral basicranium, which acts mainly as a support for the brain (Bastir and Rosas, 2006; Neaux et al., 2013). However, few studies have focused on three-dimensional (3D) variation in more lateral basicranial morphology, having mostly encompassed small evolutionary scales and ontogenetic changes in samples of modern humans and related species (e.g., Bastir et al., 2011; Neaux et al., 2013). For example, it has been suggested that the middle cranial fossae of modern humans, a region intimately related to the temporal lobes of the brain, may be characteristic of our distinct craniofacial morphology (Bastir et al., 2008). Consequently, changes in brain morphology—related or not to encephalization processes—may also be responsible for shaping morphological variation at more lateral aspects of the basicranium.

Platyrrhines, one of the three major groups of living primates, experienced a major evolutionary radiation in an isolated continent over a large temporal scale (i.e., 25–40 million years ago or megannums [Ma] in Central and South America; Perez et al., 2013). This radiation resulted in remarkable variation in body size and cranial morphology (Rosenberger et al., 2009; Perez et al., 2011; Aristide et al., 2015). Previous studies have also suggested that platyrrhines underwent several evolutionarily independent changes in relative brain size (Hartwig et al., 2011; Allen and Kay, 2012) after their early radiation (Rosenberger, 1992; Rosenberger et al., 2009; Perez et al., 2011; Aristide et al., 2015). Given the particular conditions in which their radiation occurred, platyrrhines are an excellent reference system in which to study cranial base diversification. In particular, the presence of the phylogenetically independent processes of encephalization and de-encephalization (reduction of relative brain size with respect to a putative ancestor; Hartwig et al., 2011) presents an interesting opportunity to study, on a large phylogenetic scale, the morphological correlates of primate diversification in brain size.

The aim of this study is to explore the pattern of variation in basicranial morphology in platyrrhine primates and to assess whether it is related to relative brain size. We hypothesize that similarity in basicranium shape among platyrrhine species can occur due to changes in relative brain size, independently of phylogenetic structure (i.e., basicranial shape convergence). Alternatively, if basicranial morphology of primates is related to the branching process of the species and random factors, we expect this structure to display a high and significant phylogenetic signal following a Brownian motion model of evolution (Felsenstein, 1985). To test these hypotheses, we first quantified variation in 3D shape of the inner cranial base and measured endocranial volumes (ECV) virtually in a large sample of platyrrhine species, employing high-resolution 3D CT-scans and geometric morphometric techniques (Mitteroecker and Gunz, 2009). Second, we explored the relationship between basicranial shape and relative brain size using phylogenetic regression methods (Rohlf, 2001; Freckleton et al., 2002), and calculated a measure of phylogenetic signal in the different datasets in order to assess the alternative scenarios (Blomberg et al., 2003; Adams, 2014). Finally, because previous studies have suggested that the cranial base is constituted by two separate evolutionary modules in humans and fossil and living relatives (Bastir and Rosas, 2006, 2009), we also tested the two hypotheses using separate morphometric datasets for the midline and lateral cranial base.

Materials and methods

Sample

The specimens included in this study constitute a phylogenetically informed and representative sample of platyrrhine diversity. Table 1 details the composition of the final sample of 142 skulls of both sexes from 45 species or lineages (ca. 40–60% of recognized taxa; Rosenberger and Hartwig, 2001; Groves, 2005; Aristide et al., 2015) belonging to each of the 17 broadly recognized platyrrhine genera. Each species was represented by one to six individuals. Smaller sample sizes mainly belong to species that are scarce in nature and/or in museum collections (e.g., *Callimico goeldii*). This could have an effect on the estimations of mean values for these species; however, when variation among taxa is relatively large these sample sizes are generally adequate for morphological studies (Polly, 2003; but see Cardini and Elton, 2007). In particular, in these cases it is possible to estimate the mean shape of very small samples with enough precision to accurately assess distances between species (Polly, 2003), and therefore relatively small errors in the estimation of each species mean do not greatly affect the global pattern of variation among all the species. Moreover, as this study is concerned with the global patterns of macroevolutionary change, we prioritized the sampling of a larger number of taxa, as this is an important step in obtaining a representative picture of the morphological variation exhibited by the whole clade. The taxonomy of the specimens was reassessed when possible according to their geographic location and following the IUCN Red List maps (Rylands et al., 2012; IUCN, 2014). Individuals with ambiguous locations, no geographic information, or uncertain taxonomy were excluded from the sample.

All skulls belonged to adult individuals, defined as having a completely erupted and functional dentition. The species samples are generally sex balanced, but we tested for the effect of sexual

Table 1
Species included in this study, number of specimens analyzed[a], and measured mean endocranial volumes (ECV).

Species	*n* (m,f,nd)	ECV
Alouatta belzebul	2 (1,0,1)	57.696
Alouatta caraya	6 (3,3,0)	50.784
Alouatta fusca	1 (0,1,0)	53.102
Alouatta macconelli	1 (1,0,0)	58.771
Alouatta palliata	2 (1,1,0)	48.727
Alouatta seniculus	1 (1,0,0)	54.996
Aotus azarae	2 (0,1,1)	15.164
Aotus nigriceps	4 (1,2,1)	16.673
Ateles chamek	2 (1,0,1)	105.810
Ateles geoffroyi	2 (1,1,0)	107.032
Ateles marginatus	4 (3,0,1)	122.251
Ateles paniscus	4 (1,2,1)	115.386
Brachyteles arachnoides	5 (2,0,3)	108.027
Brachyteles hypoxanthus	2 (0,0,2)	114.999
Cacajao calvus	4 (1,3,0)	69.609
Cacajao melanocephalus	3 (2,1,0)	67.966
Callicebus brunneus	3 (1,2,0)	15.462
Callicebus donacophilus	4 (3,1,0)	13.802
Callicebus moloch	4 (1,2,1)	16.924
Callicebus personatus	4 (2,2,0)	20.536
Callimico goeldii	1 (0,0,1)	10.887
Callithrix aurita	1 (0,1,0)	7.497
Callithrix jacchus	5 (2,3,0)	8.110
Callithrix kuhlii	4 (3,1,0)	8.209
Callithrix penicillata	4 (2,1,1)	7.192
Cebuella pygmaea	3 (2,0,1)	4.002
Cebus albifrons	4 (2,2,0)	71.606
Cebus nigritus	6 (3,3,0)	61.675
Chiropotes chiropotes	2 (2,0,0)	56.374
Chiropotes satanas	1 (0,0,1)	52.002
Lagothrix lagotricha	5 (1,4,0)	89.818
Leontopithecus chrysomelas	3 (1,0,2)	12.467
Leontopithecus rosalia	4 (1,2,1)	12.298
Mico argentatus	4 (3,1,0)	8.020
Mico chrysoleucus	4 (2,2,0)	7.940
Mico humeralifer	1 (1,0,0)	8.423
Pithecia irrorata	4 (1,2,1)	33.258
Pithecia monachus	3 (1,0,2)	32.918
Pithecia pithecia	3 (2,1,0)	30.509
Saguinus bicolor	2 (0,0,2)	10.013
Saguinus fuscicollis	4 (3,1,0)	7.710
Saguinus midas	5 (2,3,0)	10.824
Saguinus mystax	5 (3,2,0)	11.264
Saimiri boliviensis	4 (2,0,2)	24.866
Saimiri sciureus	2 (1,1,0)	23.993
Total	142	

[a] *n*: specifying the number of male [m], female [f], and not-determined [nd] specimens.

dimorphism on morphometric variation among species, and we found non-significant results of the interaction between taxa and sex ($F = 1.051$, $p = 0.264$). This result is in agreement with the fact that only a few platyrrhine species show evident sexual dimorphism in cranial morphology (Fleagle, 1999). The specimens are housed in Museu Nacional (MNRJ, Rio do Janeiro, Brazil), Museu de Zoologia (MZUSP, Universidade de Sao Paulo, Brazil), Museo Argentino de Ciencias Naturales (MACN, Buenos Aires, Argentina), and the Digital Morphology Museum of the Kyoto University Primate Research Institute (DMM, KUPRI).

Morphometric data acquisition

Computed tomography CT or μCT scans of skulls from MACN, MZUSP, and MNRJ were acquired. CT scans were made with a medical scanner (Philips Brilliance CT 64-slice). Pixel size ranged from 0.14 to 0.28 mm, slice thickness from 0.33 to 0.45 mm, and slice interval from 0.50 to 0.66 mm. μCT scans were performed using a table top scanner (SkyScan/Bruker, model 1173), with a 55 kV, 8 W X-ray source. Pixel size and slice thickness were between 45 and 67 μm. In order to expand our species sample, additional CT-scanned specimens were downloaded from the DMM-KUPRI repository. Pixel size of these specimens ranged from 0.10 to 0.21 mm, slice thickness was 0.5 mm for all individuals, and slice interval ranged from 0.20 to 0.50 mm. The differences in spatial resolution among the scanners did not affect the results because these differences were much smaller than the differences among specimens and the landmark digitization error. However, medical CT scans were only used for the bigger genera.

3D surface models for each skull were generated from the CT data using Slicer 4 (www.slicer.org) and saved in the PLY file format. These 3D models were subsequently edited in MeshLab (meshlab.sourceforge.net), where the upper region of the cranial vault was digitally removed to access the base of the endocranium for landmark digitization (see below).

Landmark data A total of 20 3D coordinate landmarks and 248 curve and surface semilandmarks (Fig. 1a; Table 2) were digitized by a single researcher (L.A.) on each surface model using IDAV Landmark software (Wiley et al., 2005). The landmarks allowed us to describe the relative spatial position of particular anatomical points in a structure (Bookstein, 1991). The use of semilandmarks, however, allows the characterization of anatomical regions where landmarks are absent or scarce (e.g., the surface of bones; Bookstein, 1997; Gunz and Mitteroecker, 2013). Geometric morphometric methods assume that corresponding points among specimens are homologous. In the case of landmarks, a homologous structure is considered as the point at which the landmark is located, while in the case of semilandmarks, a homologous structure is considered to be the whole curve or surface described (Perez et al., 2006; Gunz and Mitteroecker, 2013). The original information regarding the location, orientation, and scale (i.e., non-shape variation) of the configurations of landmarks and semilandmarks is not homologous among structures or individuals and, therefore, this information needs to be removed from the analyses. Moreover, the non-shape variation tangent to the curves and surfaces of semilandmarks must also be mathematically eliminated. Thus, the concept of homology behind individual landmarks and sets of semilandmarks is similar (Perez et al., 2006; Gunz and Mitteroecker, 2013).

To calculate shape variables, a Generalized Procrustes Analysis (GPA) was performed. GPA allows the removal of non-shape differences in the location, orientation, and scale of the landmark and semilandmark configurations using a least squares criterion (Rohlf

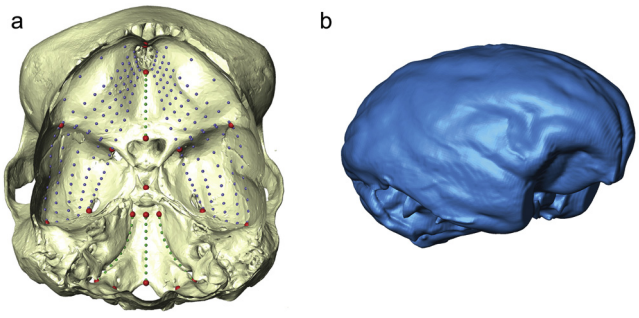

Figure 1. a) Cranial base landmarks and semilandmarks used in this study. Large red spheres: landmarks; small green spheres: curve semilandmarks; small blue spheres: surface semilandmarks. The 3D model corresponds to a *Callicebus personatus* specimen morphed into the platyrrhine sample consensus shape. b) Platyrrhine virtual cranial endocast corresponding to an *Alouatta caraya* specimen. Models are not to scale. (For interpretation of the references to colour in this figure legend, the reader is referred to the web version of this article.)

Table 2
Landmarks used in this study.

Landmark#	Landmark	Definition
1	Basion	Midpoint of the anterior margin of the foramen magnum
2	Middle spheno-occipital	Spheno-occipital suture at the midline
3	*Dorsum sellae*	Anterior edge at the midline
4	Sphenoidale	Most posterior, superior midline point of planum sphenoideum
5	Posterior "olfactory pit"	Posterior edge of the olfactory pit at the midline
6	Anterior "olfactory pit"	Anterior edge of the olfactory pit at the midline
7	Left lateral foramen magnum	Widest point, immediately above left hypoglossal canal
8	Right lateral foramen magnum	Widest point, immediately above right hypoglossal canal
9	Left superior orbital fissure	Lateral vertex
10	Left spheno-occipital	Lateral spheno-occipital suture
11	Left jugular foramen	Most posterior and inner point
12	Right superior orbital fissure	Lateral vertex
13	Right spheno-occipital	Lateral spheno-occipital suture
14	Right jugular foramen	Most posterior and inner point
15	Left spheno-parietal	At the junction
16	Left petrous-parietal	Junction of petrous part of temporal and parietal bones
17	Left foramen ovale	Posterior vertex
18	Right spheno-parietal	At the junction. Limit between anterior and middle cranial fossa.
19	Right petrous-parietal	Junction of petrous part of temporal and parietal bones
20	Right foramen ovale	Posterior vertex

and Slice, 1990). Moreover, to reduce the non-shape variation in semilandmark points, we proceeded to slide the points along tangents and tangent planes to the curves and surfaces, respectively, in order to minimize the bending energy distance among semilandmarks corresponding to each specimen and the consensus configuration (Gunz et al., 2005). After the GPA and the sliding procedure, the resulting point coordinates are Procrustes shape coordinates or shape variables. This analysis also generated Centroid Size (CS, the square root of the squared sum of the distances of each landmark and semilandmark to the geometric center of the configuration or centroid) for each specimen, which was used in the following analyses as a basicranial size variable. Two reduced datasets that consisted of a) six landmarks and 20 semilandmarks along the cranial base midline and b) eight landmarks and 208 semilandmarks comprising the lateral cranial base (i.e., middle and anterior cranial fossae) were also generated, using separate GPAs.

To reduce the dimensionality of the shape space, a Principal Components Analysis (PCA) or Relative Warps Analysis was performed on all mean Procrustes shape coordinates, or consensus shapes, for the studied species (Bookstein, 1991; Mitteroecker and Gunz, 2009). By using a singular value decomposition of the covariance matrix of species consensus shapes, the PCA generates uncorrelated axes that describe the major trends in shape variation among species. These axes are linear combinations of the original Procrustes coordinates derived from a rigid rotation of the shape space, which ensures that it is not deformed in the process (Mitteroecker and Gunz, 2009). The first PCs can also be interpreted as the dimensions that best reproduce the Euclidean distances among species. Thus, the PC scores were used in subsequent analyses as variables representing the platyrrhine major shape variation patterns. To visualize the shape changes along the PCs, a 3D surface model of the Procrustes mean configuration was warped along the first two principal component axes using a thin-plate spline (TPS) interpolation (Wiley et al., 2005).

Seventeen specimens (one from each genus) were measured twice in different events three weeks apart from each other using IDAV Landmark software (Wiley et al., 2005), and a GPA, a sliding semilandmark procedure and a PCA were performed independently for the two datasets generated in each measurement event. To evaluate the importance of observational error in the following statistical analyses, the patterns of ordination produced by the PCA for the two series of observations were compared using a PROTEST analysis (Peres-Neto and Jackson, 2001). First, this analysis uses a Procrustes method to scale and rotate the ordinations, using a least squares criterion. Then, the standardized sum of the squared residuals between both ordinations after the superimposition was used as a measure of association. Finally, a permutation procedure (PROTEST) was used to assess the statistical significance of the procrustean fit (Peres-Neto and Jackson, 2001). The results showed significant similarities between the two series of observations (Procrustes correlation = 0.98, $p = 0.001$). All morphometric analyses were conducted with R (R Core Team, 2014) and the geomorph package (Adams and Otárola-Castillo, 2013) for R.

Endocranial volume (ECV) measurement To obtain a precise estimation of the relationship between skull shape and ECV, the ECV of each specimen was measured. This also allowed us to incorporate species with no measurements available in the previous works and to have a full correspondence between the morphometric and ECV data. To measure the ECV, virtual endocasts were generated from the CT slice data (Neubauer et al., 2009) using a threshold-based 2D segmentation procedure in ITK-SNAP 3.0 (Yushkevich et al., 2006). A threshold gray value was defined that clearly separated bone from air. When present, foramina were virtually closed in each slice to allow the threshold segmentation procedure. Finally, a surface 3D model—a virtual endocast—was generated for each specimen from the segmented volume corresponding to the endocranium (Fig. 1b), and the volume enclosed by the surface was measured in Meshlab.

The differences in slice number among the different sources for the CT scans may affect the measured volume. Several μCT scans were downsampled to match the number of slices in those CT scans with less resolution, and the obtained ECV was compared to that measured with full resolution. The differences were less than 1% and most likely attributable to the procedure of manually closing the foramina. Thus, all μCT specimens were downsampled to a reasonable number of slices for segmentation, ensuring that the final result remained unaffected.

Our data expand the primate ECV dataset of Isler et al. (2008), adding 18 platyrrhine species. Our ECV estimations were compared with the 27 species previously published by Isler et al. (2008), and we found a high and significant Pearson correlation ($r = 0.993$; $p < 0.001$). Therefore, the resulting estimations from the virtual ECV measurement protocol can be considered as reliable as the direct measurements of Isler et al. (2008; see Discussion). Given

that our main objective was to have a precise estimation of the relationship between ECV and cranial shape for the 142 individuals and 45 species included in our study, our virtual ECV estimations were used in the following analyses.

Phylogenetic comparative analyses

First, to examine the relationship between the phylogeny of the platyrrhines and their pattern of phenotypic variation, a measure of the phylogenetic signal in several traits was estimated (i.e., shape variables, log CS, log Body Mass [BM], log ECV, and residual log ECV [see below]). Phylogenetic signal is the tendency for closely related species to be more similar in a given trait than more distant ones, or alternatively, a measure of statistical dependence of trait values among tips in a phylogenetic tree. Blomberg's K statistic (Blomberg et al., 2003) was calculated, which provides a metric of the strength of phylogenetic signal for univariate data. This statistic is computed as K = observed (MSE_0/MSE)/expected (MSE_0/MSE), where MSE_0 is the mean square error of trait values measured from the phylogenetic mean, and MSE is the same as MSE_0 but first correcting for phylogenetic non-independence. The denominator is the expected MSE ratio under a Brownian motion (BM) model of character evolution. K values near 0 indicate a lack of signal, while values near 1 are expected under BM. Values above 1 are indicative of a stronger association between the phylogeny and the character under study than expected under BM, for example, as observed in early niche filling scenarios (see Revell et al., 2008). For multidimensional data (e.g., Procrustes shape coordinates), a multivariate extension of the K statistic, Kmult, was calculated, which has the same expected values as its univariate counterpart (Adams, 2014). Significance values for phylogenetic signal were obtained via permutations of the data among the tree tips (Blomberg et al., 2003; Adams, 2014).

Phylogenetic relationships among platyrrhine species were obtained from a fossil-calibrated Bayesian tree generated by Aristide et al. (2015) using a concatenated dataset of 25,361 DNA base pairs containing several coding and non-coding sequences. The phylogenetic signal was calculated using the picante (Kembel et al., 2010) and geomorph (Adams and Otárola-Castillo, 2013) packages for R.

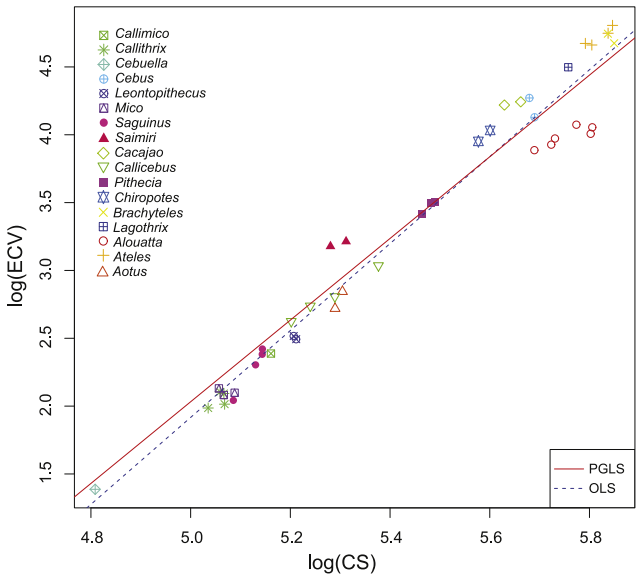

Figure 2. Phylogenetic generalized least squares (PGLS) and ordinary least squares regressions of log CS against log ECV values at the species level. Residuals from the PGLS regression were used in further analyses as a measure of relative brain volume or encephalization degree (residual-ECV).

Second, to assess the association between encephalization and basicranial morphology (size and shape), a series of Phylogenetic Generalized Least Squares (PGLS; Martins and Hansen, 1997; Rohlf, 2001) regression models were employed. These models take into account the expected lack of independence among samples arising from phylogenetic structure. In Ordinary Least Squares (OLS) models, the error term is assumed to be independent and is therefore represented by the identity matrix; in contrast, in PGLS models, covariation in the error term structure is modeled by incorporating phylogenetic relationships as a covariance matrix derived from the phylogenetic tree, its branch lengths, and a model of character evolution, most commonly Brownian motion. Initially, log ECV was fitted to log CS (as a measure of basicranial size) to correct for allometric scaling. This allowed us to generate residual-ECV values (measured as the distance from each observation to its expected value given the regression line) that were subsequently used as a measure of relative brain size or encephalization index. This residual-ECV measurement differs from previous platyrrhine estimations that used body mass as a correction factor (Hartwig et al., 2011; Allen and Kay, 2012) and is explicitly designed to explore the association between basicranial morphology and relative brain size (see Ross and Ravosa, 1993). Consequently, to explore the relationship between encephalization and basicranial morphology, basicranial shape variables (as Principal Components) were fitted, using PGLS regressions, to these residual-ECV values.

Finally, to visualize changes in encephalization along the phylogeny, the residual-ECV values were mapped and plotted onto the platyrrhine tree using an ancestral character state reconstruction procedure based on a maximum likelihood approach (Schluter et al., 1997; Revell, 2013). Under this approach, the character is assumed to have evolved under a Brownian motion process, where the expected difference between any two species is proportional to the time since their last common ancestor (Felsenstein, 1985). This way, the character state at nodes can be calculated by minimizing the squared sum of changes along the branches of the tree (McArdle and Rodrigo, 1994). Character states along branches are calculated by interpolation of values between nodes (Revell, 2013). Although uncertainty in point estimates can be high, particularly at basal nodes (Schluter et al., 1997), this tool can be useful for visualizing the directionality of evolutionary changes at more recent nodes in a phylogeny (Revell, 2013).

PGLS and ancestral character reconstruction analyses were conducted using the caper (Orme, 2013) and phytools (Revell, 2012) packages for R.

Results

Endocranial volume

We measured the ECV for a total of 142 adult skulls belonging to 45 different species (Fig. 1b). Table 1 shows the mean ECV values and the number of specimens for each species. The regression analyses between log CS and log ECV showed that endocranial volume is strongly and significantly associated with cranial base size (Fig. 2), even when taking into account the phylogenetic structure of the data (PGLS coefficient = 3.009, Lambda = 0.997, $R^2 = 0.89$, $F_{1,43} = 332.7$, $p = 0.000$). The residual-ECV values from the PGLS analysis are mapped onto the phylogeny of Fig. 3. *Alouatta* showed a noticeably lower residual-ECV for its basicranial size, while three clades—pithecines (*Chiropotes* and *Cacajao*), cebines (*Cebus* and *Saimiri*), and atelines (*Lagothrix*, *Brachyteles*, and *Ateles*)—showed phylogenetically independent increases in their residual-ECV. The K values for both log ECV and residual-ECV indicated a high and significant phylogenetic signal (Table 3). For comparative purposes, we analyzed the relationship between log body mass (BM; data

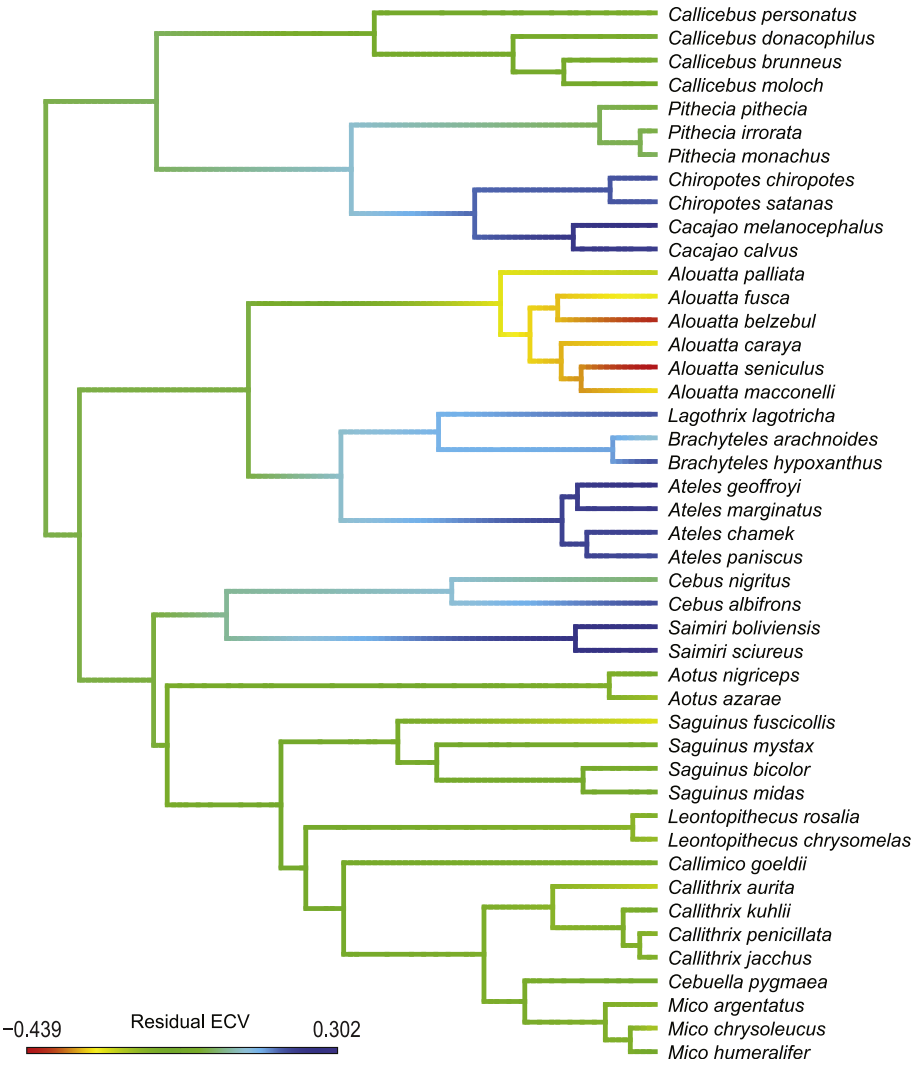

Figure 3. Relative brain size (estimated as residual ECV; see methods) of the studied platyrrhine species mapped on the phylogeny. Values at nodes and branches were reconstructed using a maximum likelihood ancestral character estimation method. The tree is from Aristide et al. (2015).

Table 3
Phylogenetic signal for cranial size (log CS) and shape, body mass (log BM), and endocranial volume (ECV and residual-ECV) as measured by K (Blomberg et al., 2003) and Kmult (Adams, 2014) statistics and their associated significance p values obtained by permutation tests.

		K	p
Size and Brain data			
	log CS	3.911	0.0001
	log BM	3.858	0.0001
	log ECV	4.097	0.0001
	Residual ECV	1.370	0.0001
Shape data			
	PC1	1.056	0.0001
Complete dataset	PC2	1.663	0.0001
	Whole shape	0.564	0.0001
	PC1	1.270	0.0001
Midline	PC2	0.911	0.0001
	Whole shape	0.636	0.0001
	PC1	1.179	0.0001
Lateral	PC2	0.994	0.0001
	Whole shape	0.576	0.0010

from Smith and Jungers (1997) and Isler et al. (2008)) and our log ECV. The PGLS result showed a strong and significant association between these variables (PGLS coefficient = 0.70, R^2 = 0.75, $p < 0.01$, *n* species = 45), which is similar to the results of previous studies (PGLS coefficient = 0.66, $R^2 = 0.74$, $p < 0.01$, *n* species = 37; Allen and Kay, 2012).

Morphometric variation

Fig. 4 shows the basicranial shape distances among platyrrhine species in the plane defined by the first two principal component (PC) axes for the complete dataset. PC1 and PC2 represent 62.7% of the total shape variation (32.7% and 30.0%, respectively; see also SOM Fig. 1). A clear separation between the Atelidae + Pitheciidae versus Cebidae clades is observed, with some overlap between the Pitheciidae and the Atelidae. Noticeably, *Aotus* species fall closer to the Pitheciidae clade in both datasets. *Alouatta* and *Saimiri* appear as extremes of variation in shape characteristics in both datasets; *Ateles* and *Leontopithecus* show a comparable amount of dissimilarity in the complete dataset.

The shape changes associated with PC1 and PC2 in the complete dataset are shown in Fig. 5 and in the SOM 3D models, which can be

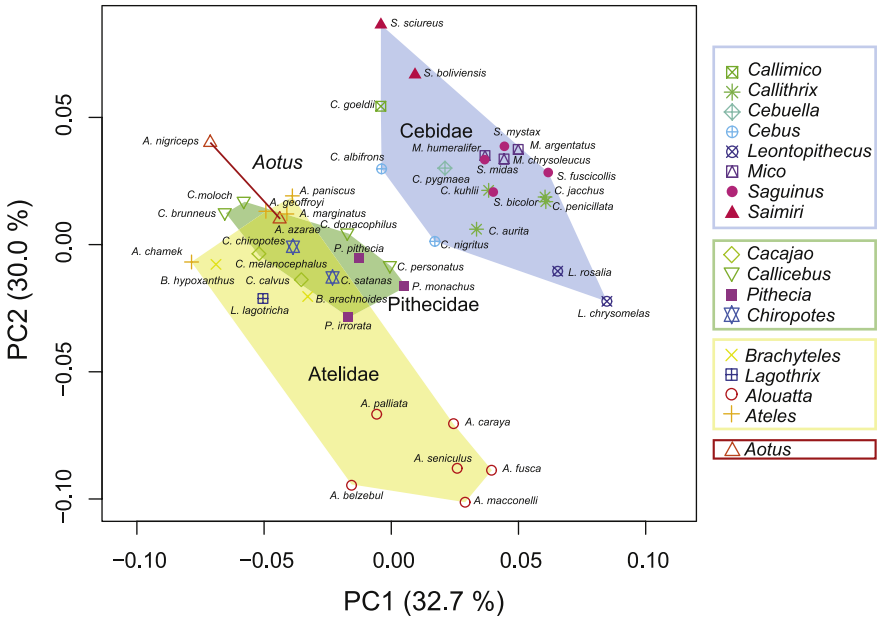

Figure 4. Ordination of the mean shape of the 45 platyrrhine species studied in the space defined by the first two principal components of basicranial shape variation for the complete dataset.

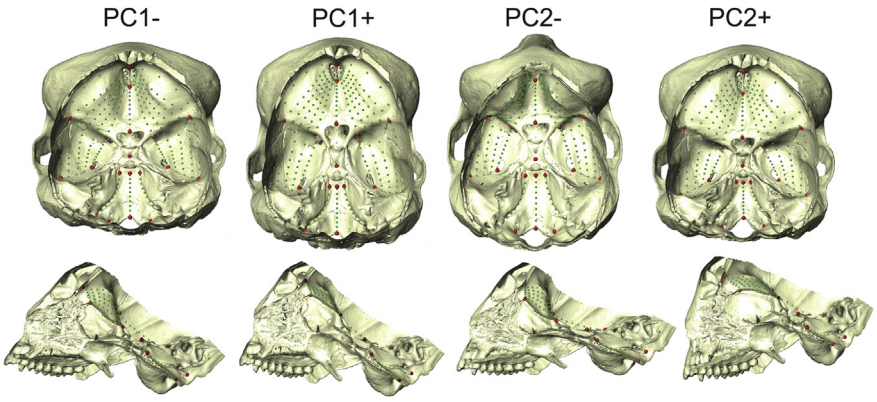

Figure 5. Shape changes associated with PC1 and PC2 of the complete dataset. Superior (top) and midline (bottom) endocranial views. The images were obtained by warping a surface model of the mean platyrrhine basicranial shape along the major axis of shape change or PCs scores.

visualized in Meshlab. PC1 is mainly associated with the relative length and width of the cranial base, being short and wide in the negative direction. There is also a deepening of the middle area at the anterior cranial fossae in relation to the orbital roof but with no increased dorsoventral flexion (Fig. 5). PC2, which explains a similar amount of variation as PC1, is related to flexion of the midline but also to deeper and relatively shorter middle cranial fossae in the positive direction. This pattern also extends to the basilar part of the occipital bone, which is relatively shorter (Fig. 5).

Fig. 6 shows the basicranial shape distances among platyrrhine species in the plane defined by the first two principal component (PC) axes, both for the midline dataset (Fig. 6a) and the dataset of the lateral structures (Fig. 6b). For the midline dataset, PC1 accounts for 51.2% and PC2 for 20.7% of total shape variation. For the lateral dataset, PC1 and PC2 represent 67% of the total shape variation (40.5% and 26.5%, respectively). In both cases, the main direction of dispersion of the species in the shape space of the first two PCs is similar to the pattern observed in the complete dataset.

The shape changes associated with PC1 and PC2 in both the midline and lateral datasets are shown in Fig. 7 and in the SOM 3D models. For the midline dataset, PC1—the main dimension of shape variation—is mainly associated with the degree of flexion of the midline. PC2 shows changes associated with the relative length of the olfactory pit and the midline anterior cranial fossae (Fig. 7a). For the lateral dataset, PC1 is mainly associated with the relative length and width of the cranial base, being short and wide in the negative direction (Fig. 7b). PC2 of the lateral dataset mainly shows deeper and shorter middle cranial fossae and less protruding orbital roofs, in the positive direction (Fig. 7b).

Phylogenetic signal test results are shown in Table 3. For the three shape datasets, PCs 1 and 2 individually showed clear and significant phylogenetic signals whose K values were approximately those expected under a Brownian motion model of character evolution. When the whole-shape variables were considered together, a weaker but highly significant phylogenetic signal was found. Thus, these results highlight the importance of phylogenetic structure or branching pattern for understanding platyrrhine

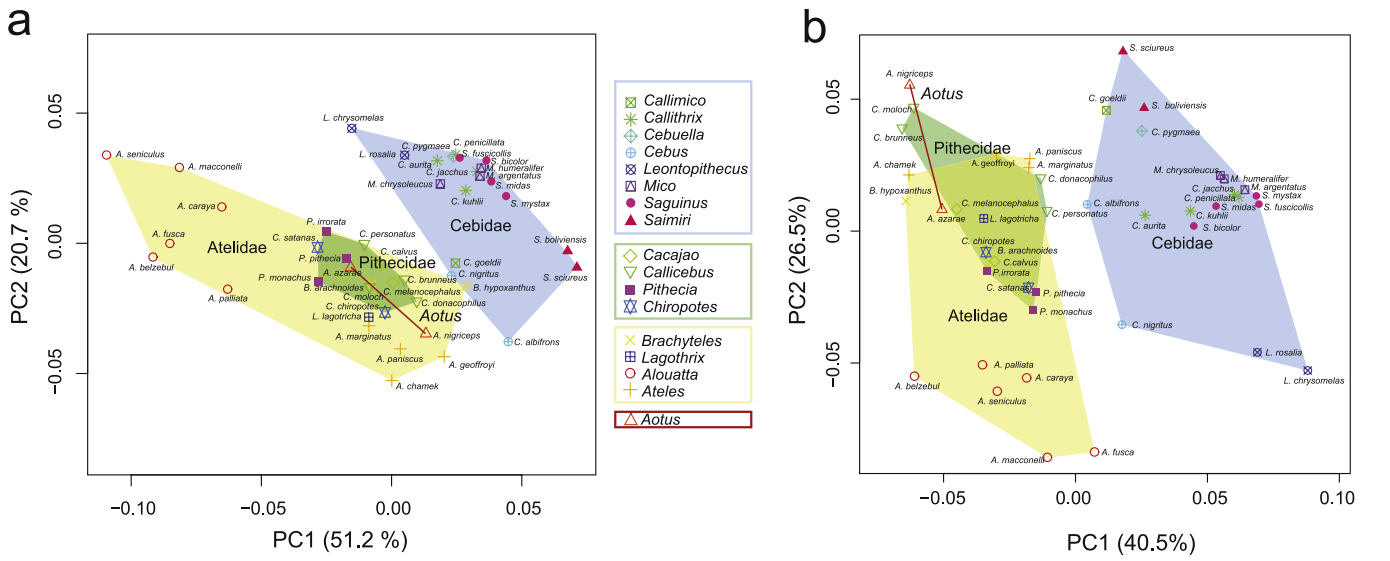

Figure 6. Ordination of the mean shape of the 45 platyrrhine species studied in the space defined by the first two principal components of basicranial shape variation for the (a) midline and (b) lateral datasets.

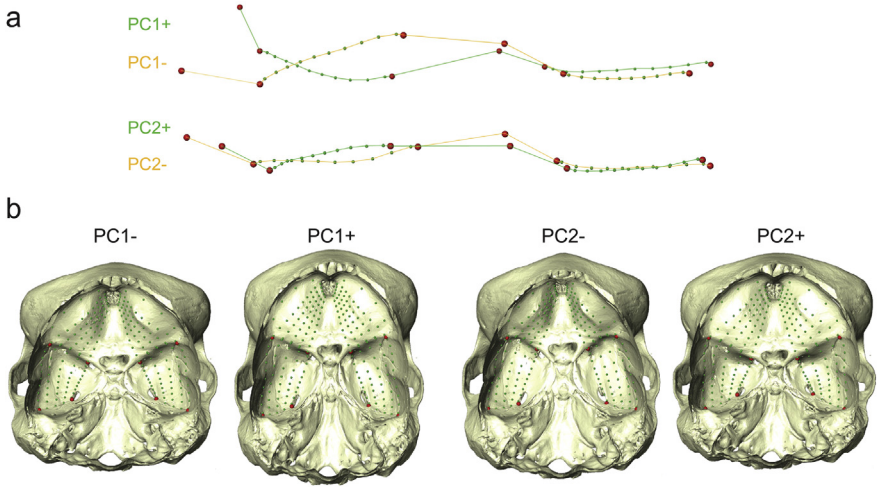

Figure 7. Shape changes associated with PC1 and PC2 for the (a) midline and (b) lateral datasets. The images were obtained by changing wireframe graphs and warping a surface model of the mean platyrrhine shape along the major axis of shape change or PCs scores.

Table 4
Phylogenetic regression analyses (PGLS) for shape data versus residual-ECV values (see text). Regression parameters are shown.[a]

	Data	Lambda	R^2	F (1/43)	p
Complete dataset	PC1	0.926	0.1278	6.30	0.0159
	PC2	0.988	0.2545	14.68	0.0000
	PC1-2	0.945	0.0022	0.10	0.7572
	PC1-9	0.869	0.0113	0.49	0.4873
Midline	PC1	0.950	0.4878	40.96	0.0000
	PC2	0.864	0.2181	12.00	0.0012
	PC1-2	0.965	0.1489	7.52	0.0089
	PC1-5	0.928	0.0346	1.54	0.2214
Lateral	PC1	0.949	0.0033	0.14	0.7063
	PC2	0.954	0.1580	8.07	0.0068
	PC1-2	1.000	0.0624	2.86	0.0980
	PC1-8	0.866	0.0062	0.27	0.6083

[a] All λ values were estimated by maximum likelihood, and results were not significantly different from 1.

basicranial shape diversification. However, in all cases, the K values for shape variation were lower than those estimated for log CS, log BM, and log ECV, which showed an even higher phylogenetic signal (Table 3).

Relationship between basicranial shape and encephalization

The results of the phylogenetic regressions between the basicranial shape variables and the residual ECV, or encephalization, are shown in Table 4. In all cases, the lambda branch length transformation parameters of the PGLS analyses were not significantly different from 1 (results not shown). This indicated that the phylogenetic structure in the data can be accounted for using a Brownian motion model of evolution. For the complete dataset, the PGLS analyses showed that the residual-ECV explained ca. 25% of the variation for PC2 but only ca. 13% for PC1; both displayed significant association values. However, the multivariate regression of PC1 plus PC2 and PC1 to PC9 (which accounted for 90% of the total shape variation) on residual-ECV explained ca. 1% and showed no

significant results. Conversely, for the midline, the analyses showed a stronger association between the residual-ECV and PC1 and PC2 compared to the complete dataset. Encephalization explained up to 48% of the variation in PC1, 22% of PC2, and 15% of PC1 plus PC2, all of which were significant. No significant association was found in the multivariate regression of PC1 to PC5 (90% of total midline shape variation) on the residual-ECV. For the lateral dataset, the analyses showed that the residual-ECV explained ca. 16% of the shape variation for PC2 but ca. 0% for PC1. No significant association was found in the multivariate regression of PC1 and PC2 and of PC1 to PC8 (90% of total midline shape variation) on the residual-ECV. Finally, as previous works have suggested a strong relationship between platyrrhine skull shape and size (Marroig and Cheverud, 2001, 2005), we tested the association of basicranial Procrustes shape variables with log CS and found a low correlation (Complete dataset, first 9 PCs: PGLS coefficient = −0.01, $R^2 = 0.03$, p = 0.21, *n* species = 45; Midline dataset, first 5 PCs: PGLS coefficient = −0.01, $R^2 = 0.04$, p = 0.16, *n* species = 45; Lateral dataset, first 8 PCs: PGLS coefficient = −0.13, $R^2 = 0.21$, p = 0.001, *n* species = 45).

Discussion

Previous studies have suggested that platyrrhine primates likely underwent several evolutionarily independent increases in relative brain size or encephalization processes (Isler et al., 2008; Hartwig et al., 2011; Allen and Kay, 2012). We will first discuss our results on the pattern of variation of endocranial volumes that were independently estimated from a large sample of platyrrhine species, employing high-resolution 3D CT-scans. Finally, we will discuss the morphological correlates of variation in relative brain size among platyrrhines. In particular, we will return to the main objectives of this study: characterizing the pattern of basicranial shape variation in platyrrhines and assessing its relationship with relative brain size variation.

Brain size evolutionary variation

In agreement with a previous study (Hartwig et al., 2011), we found a brain size variation pattern that agrees with the hypothesis that at least three platyrrhine clades likely underwent phylogenetically independent encephalization processes: pitheciines (*Chiropotes* and *Cacajao*), cebines (*Cebus* and *Saimiri*), and atelines (*Lagothrix*, *Brachyteles*, and *Ateles*). In particular, *Saimiri*, *Ateles*, and *Cacajao* appear to be the most encephalized platyrrhines within their respective lineages. Conversely, *Alouatta*, the sister clade of atelines, shows a remarkable de-encephalized phenotype relative to the hypothetical ancestral state.

A particular focus has been placed on the quality of primate brain size datasets. For example, the use of captive individuals, small sample sizes, changing taxonomy, and the combination of data obtained using different methods have been mentioned as potential bias sources (Healy and Rowe, 2007; Isler et al., 2008). However, our brain size dataset appears to overcome these potential problems. First, although we combine wild and a few captive individuals, Isler et al. (2008) showed that endocranial volume (ECV) measurements did not differ between these categories, even when body mass exhibited high variation levels. Second, we only measured each of the included specimens in the morphometric dataset, avoiding the use of brain size data collected from different sources. Third, taxonomy was carefully reassessed using collection locality and known geographic ranges for the wild specimens. Finally, our virtual ECV measurements are highly correlated with the dry-crania direct measurements of Isler et al. (2008), and our regression slope between ECV and body mass for platyrrhines is similar to that obtained by Allen and Kay (2012; 0.70 versus 0.66).

In our study, encephalization was measured as the residual values from a phylogenetic regression of ECV versus basicranial size. This measure is different from that of previous platyrrhine studies, which corrected for body mass (e.g., Hartwig et al., 2011; Allen and Kay, 2012; van Woerden et al., 2014). Thus, we avoided the use of body mass data from external sources, which may introduce severe bias to the analyses, and generated an encephalization measure that is based completely on the studied specimens. Moreover, and most importantly, this method generates a more appropriate quantification of brain size increase in a morphological context because it is measured relative to the brain support structure, i.e., the cranial base. For example, Ross and Ravosa (1993) used a basicranial length measure to estimate residual ECV values in their basicranial variation study. However, as the brain is a three-dimensional structure, considering both length and width of the cranial base would constitute a more suitable size measure in the context of the spatial packing model (Lieberman et al., 2008). In this sense, the use of geometric morphometric methods readily provided us with a size variable—centroid size—that derives from the whole structure under study, thus providing a better measurement with respect to the brain support structure than traditional linear measurements.

Several factors that may drive or constrain changes in relative brain size in primates have been proposed (e.g., group size, foraging strategy, gut size, and maternal energy investment) and extensively investigated (e.g., Dunbar, 1995; Aiello and Wheeler, 1995). However, platyrrhines have not received much attention in brain size evolution studies, despite their notable characteristics. Investigating the role of energetic constraints, Hartwig et al. (2011) and Allen and Kay (2012) showed that diet quality and gut size do not correlate with relative brain size in platyrrhines, whereas van Woerden et al. (2014) indicated a negative relationship with seasonal fluctuations in diet composition. These results are therefore inconclusive regarding the role of energetic constraints in brain size evolution in this clade of primates. Conversely, Hartwig et al. (2011) suggest a relationship of brain size with group size and foraging strategy among platyrrhines, but these hypotheses were not formally tested. Therefore, more studies are needed in order to understand the mechanisms and factors involved in platyrrhine brain evolution.

Encephalization and cranial base shape variation

Our results show that platyrrhines exhibit a high degree of basicranial shape variation. This is mainly represented as a disparity in basicranial flexion at the midline: the relative width and length of the whole cranial base (which are inversely associated), and the relative depth of the middle cranial fossae. Among these changes, the midline cranial base region displays the most consistent pattern, mainly varying in its degree of dorsoventral flexion (Figs. 6 and 7; SOM 3D models), which is in concordance with other primate comparative studies (e.g., Ross and Ravosa, 1993; Bastir et al., 2010).

Even though platyrrhines present a high variation in relative brain size (Fig. 3), results show that encephalization has only a limited effect on the main axes of basicranial shape variation. Phylogenetic regressions show that, for the whole cranial base dataset, this effect, although significant, is not very strong. Only 12% of the morphological variation in PC1 and 25% in PC2, the axis describing basicranial flexion, can be explained by changes in relative brain size. Therefore, in platyrrhines, the midline is the only trait that shows a high association with encephalization, with up to ca. 48% of variation in PC1, which mainly describes basicranial flexion. Previous evolutionary studies in primates have interpreted basicranial flexion as a mechanism for spatial packing, allowing for

a larger relative brain to fit the endocranial cavity (e.g., Ross and Ravosa, 1993; Bastir et al., 2010). Therefore, expansion in brain size could be a significant factor behind midline basicranial flexion in platyrrhines, as was observed in other primate clades.

Conversely, less is known about variation in the lateral cranial base among primates, which has only recently been studied, mostly for the human clade and closely related taxa (Bastir and Rosas, 2009; Neaux et al., 2013). In spite of the observed variation in relative brain size in platyrrhines, our results show that encephalization is not related to the main axes of variation in the lateral cranial base, that is, length and width of the anterior and middle cranial fossae and depth of middle cranial fossae and orbital roof morphology. This is in line with previous work suggesting that the midline basicranium and the more lateral aspects may vary independently during evolution (e.g., Bastir and Rosas, 2006). Although we did not explicitly test this hypothesis, the PGLS results together with the fact that the midline cranial base and the more lateral aspects are each included in different, uncorrelated axes of variation in the principal component analysis shown in Fig. 4 are indicative that these two basicranial regions may behave as separate evolutionary modules (Klingenberg, 2008).

Several past studies have related lateral basicranial variation to brain size and shape. Bastir and Rosas (2009), in a study including hominins and chimpanzees, proposed modularization of midline and lateral aspects of the cranial base as a mechanism that would allow the evolution of a support structure for large brains, even when flexion at the midline remained relatively constant. Other studies suggested that lateral basicranial morphology may be directly affected by the shape (Bastir et al., 2008) or both shape and size (Neaux et al., 2013) of the brain. Alternatively, lateral basicranium morphology may be related to the variation in face and mandible morphology associated with dietary differences (Neaux et al., 2013). Our results indicate that species that exhibit convergence in their relative brain size do not display convergence in lateral basicranial shape. Thus, given the absence of a relationship between relative brain size and lateral basicranial morphology in platyrrhines, alternative explanations for the observed variation may be necessary.

Because most previous studies were focused on *Homo sapiens* and its close relatives (Ross and Henneberg, 1995; Bastir et al., 2008; Neaux et al., 2013), the importance of phylogenetic structure in cranial base variation has not been thoroughly explored before. Therefore, our phylogenetic signal analyses highlight the importance of phylogenetic history in shaping the observed patterns of basicranial variation. Moreover, we show that this is the main dimension behind cranial base variation, as was previously shown for other regions of the platyrrhine skull (Perez et al., 2011). In contrast to body mass, cranial base size, and ECV, all analyzed aspects of basicranial shape broadly evolved according to a Brownian motion model, as indicated by the K statistic.

However, our results on the variation among the main platyrrhine clades—Cebidae, Pitheciidae, and Atelidae—show that while each main clade occupies a distinct region of the morphospace, with some overlap between the Atelinae and Pitheciidae (Figs. 4 and 6), variation within clades follows similar patterns: the major direction of shape changes in the cranial base is principally related to flexion in the midline and the relative depth of the middle cranial fossae. Together, these results suggest a broader picture: while the major patterns of basicranial shape variation are phylogenetically structured, the intra-clade covariation pattern is broadly similar among clades, suggesting that common developmental and evolutionary processes are responsible for basicranial shape diversification.

Our results also show that *Aotus* exhibits a close morphological similarity to *Callicebus* and the Pitheciidae clade. This is in contrast to most molecular phylogenies, which place *Aotus* in the Cebidae clade (e.g., Opazo et al., 2006; Wildman et al., 2009; Perelman et al., 2011). However, clade support for *Aotus* as a cebid has been consistently low in these types of analyses (Perez et al., 2012). Conversely, our results align well with previous morphological assessments of the position of *Aotus* in platyrrhine phylogeny as a sister clade of *Callicebus* (Rosenberger and Tejedor, 2013), and contributes evidence based on a previously unexplored skull region to this longstanding debate. Similarly, molecular phylogenies suggest a close relationship between Atelidae and Cebidae, but we found a close similarity between Atelidae and Pitheciidae. Again, morphological phylogenies agree with this relationship (Rosenberger, 2002). The causes for the discrepancy between gene- and morphology-based trees in platyrrhines are far from clear but could be related to processes such as selection or incomplete lineage sorting, among others, which could be characteristic of the early stages of the platyrrhine radiation (Rosenberger, 1992; Perez et al., 2011, 2012; Aristide et al., 2015).

Conclusions

The main conclusion of this work, contrary to our expectations, is that the phylogenetic structure is the most important dimension for understanding shape variation in the platyrrhine cranial base. Given the importance of a Brownian motion model to describe cranial base shape variation, random factors such as genetic drift acting during the platyrrhine branching process could have been the main drivers of morphological diversification in this clade. However, basicranial differences among the main clades could be related to the retention of ancestral characteristics over time (i.e., phylogenetic conservatism; Wiens et al., 2010), which has also been suggested for other morphological variables in platyrrhines (Perez et al., 2011; Aristide et al., 2015). The factors generating this phylogenetic conservatism could include stabilizing selection, genetic, developmental, or functional constraints, and a lack of genetic variation (Gavrilets and Losos, 2009; Wiens et al., 2010; Perez et al., 2011).

For platyrrhines, encephalization was only correlated with the main axis of shape variation in the midline basicranium, i.e., the axis describing basicranial flexion. This result supports previous hypotheses suggesting that encephalization is the main factor shaping similarity in midline basicranium morphology among species derived from clades with different ancestral trait values, i.e., experiencing phenotypic convergence (Ross and Ravosa, 1993; Bastir et al., 2010). Conversely, we have shown that encephalization alone is not responsible for shaping morphological variation in more lateral aspects of the basicranium in platyrrhine primates. The evolution of basicranial variation in primates is most likely more intricate than is commonly believed, and its understanding will require further studies exploring the complex interactions between relative brain size, brain shape, cranial base morphology, and the ecological dimensions acting along the species divergence process.

Acknowledgments

We thank J. A. de Oliveira (Museu Nacional, Rio de Janeiro, Brazil), D. Flores (Museo Argentino de Ciencias Naturales "Bernardino Rivadavia", Argentina), M. de Vivo (Museu de Zoologia, Universidade de Sao Paulo, Brazil), and the Digital Morphology Museum (DMM, KUPRI, Primate Research Institute, Kyoto University, Japan) for granting us access to the platyrrhine skeletal collections under their care. We are indebted to the anonymous reviewers and JHE Editors who contributed greatly to improving the manuscript. This research was supported by Grants from the FONCyT (PICT-2011-0307), Conselho Nacional de Desenvolvimento

Científico e Tecnológico, and Fundação de Amparo à Pesquisa do Estado de São Paulo.

Appendix A. Supplementary data

Supplementary data related to this article can be found at http://dx.doi.org/10.1016/j.jhevol.2015.02.003.

References

Adams, D.C., 2014. A generalized K statistic for estimating phylogenetic signal from shape and other high-dimensional multivariate data. Syst. Biol. 63, 685–697.

Adams, D.C., Otárola-Castillo, E., 2013. geomorph: an R package for the collection and analysis of geometric morphometric shape data. Methods Ecol. Evol. 4 (4), 393–399.

Aiello, L.C., Wheeler, P., 1995. The expensive-tissue hypothesis: the brain and the digestive system in human and primate evolution. Curr. Anthropol 199–221.

Allen, K.L., Kay, R.F., 2012. Dietary quality and encephalization in platyrrhine primates. Proc. R. Soc. B Biol. Sci. 279 (1729), 715–721.

Aristide, L., Rosenberger, A.L., Tejedor, M.F., Perez, S.I., 2015. Modeling lineage and phenotypic diversification in the New World monkey (Platyrrhini, Primates) radiation. Mol. Phylogenet. Evol. 82, 375–385.

Bastir, M., Rosas, A., 2006. Correlated variation between the lateral basicranium and the face: a geometric morphometric study in different human groups. Arch. Oral Biol. 51, 814–824.

Bastir, M., Rosas, A., 2009. Mosaic evolution of the basicranium in *Homo* and its relation to modular development. Evol. Biol. 36, 57–70.

Bastir, M., Rosas, A., Lieberman, D.E., O'Higgins, P., 2008. Middle cranial fossa anatomy and the origin of modern humans. Anat. Rec 291, 130–140.

Bastir, M., Rosas, A., Stringer, C., Manuel Cuétara, J., Kruszynski, R., Weber, G.W., Ross, C.F., Ravosa, M.J., 2010. Effects of brain and facial size on basicranial form in human and primate evolution. J. Hum. Evol. 58, 424–431.

Bastir, M., Rosas, A., Gunz, P., Peña-Melian, A., Manzi, G., Harvati, K., Kruszynski, R., Stringer, C., Hublin, J.-J., 2011. Evolution of the base of the brain in highly encephalized human species. Nat. Commun 2, 588.

Biegert, J., 1957. Der Formwandel des Primatenschädels und seine Beziehungen zur ontogenetischen Entwicklung und den phylogenetischen Spezialisationen der Kopforgane. Ggbrs. Morphol. Jahrb 98, 77–199.

Biegert, J., 1963. The evaluation of characteristics of the skull, hands and feet for primate taxonomy. In: Washburn, S.L. (Ed.), Classification and human evolution. Aldine Publishing Co., Chicago, pp. 116–145.

Blomberg, S.P., Garland, T., Ives, A.R., 2003. Testing for phylogenetic signal in comparative data: behavioral traits are more labile. Evolution 57, 717–745.

Bookstein, F.L., 1991. Morphometric tools for landmark data: geometry and biology. Cambridge University Press, Cambridge.

Bookstein, F.L., 1997. Landmark methods for forms without landmarks: morphometrics of group differences in outline shape. Med. Image Anal 1, 225–243.

Bookstein, F.L., Gunz, P., Mitterœcker, P., Prossinger, H., Schæfer, K., Seidler, H., 2003. Cranial integration in *Homo*: singular warps analysis of the midsagittal plane in ontogeny and evolution. J. Hum. Evol. 44, 167–187.

Bruner, E., Martin-Loeches, M., Colom, R., 2010. Human midsagittal brain shape variation: patterns, allometry and integration. J. Anat 216, 589–599.

Cardini, A., Elton, S., 2007. Sample size and sampling error in geometric morphometric studies of size and shape. Zoomorphology 126, 121–134.

Cheverud, J.M., 1996. Developmental integration and the evolution of pleiotropy. Am. Zool 36, 44–50.

Dunbar, R.I., 1995. Neocortex size and group size in primates: a test of the hypothesis. J. Hum. Evol. 28, 287–296.

Felsenstein, J., 1985. Phylogenies and the comparative method. American Naturalist 1–15.

Fleagle, J.G., 1999. Primate Adaptation and Evolution, 2nd ed. Academic Press, New York.

Freckleton, R.P., Harvey, P.H., Pagel, M., 2002. Phylogenetic analysis and comparative data: a test and review of evidence. Am. Nat 160, 712–726.

Gavrilets, S., Losos, J.B., 2009. Adaptive radiation: contrasting theory with data. Science 323 (5915), 732–737.

Gould, S.J., 1977. Ontogeny and phylogeny. Harvard University Press, Cambridge, MA.

Groves, C., 2005. Order Primates. In: Wilson, D.E., Reader, D.M. (Eds.), Mammal Species of the World: A Taxonomic and Geographic Reference. Johns Hopkins University Press, Baltimore, pp. 111–184.

Gunz, P., Mitteroecker, P., 2013. Semilandmarks: a method for quantifying curves and surfaces. Hystrix 24, 103–109.

Gunz, P., Mitteroecker, P., Bookstein, F.L., 2005. Semilandmarks in three dimensions. In: Slice, D.E. (Ed.), Modern morphometrics in physical anthropology. Springer, New York, pp. 73–98.

Hallgrímsson, B., Lieberman, D.E., 2008. Mouse models and the evolutionary developmental biology of the skull. Integr. Comp. Biol. 48, 373–384.

Hartwig, W., Rosenberger, A.L., Norconk, M.A., Owl, M.Y., 2011. Relative brain size, gut size, and evolution in New World monkeys. Anat. Rec 294, 2207–2221.

Healy, S.D., Rowe, C., 2007. A critique of comparative studies of brain size. Proc. R. Soc. B 274, 453–464.

Isler, K., Christopher Kirk, E., Miller, J., Albrecht, G.A., Gelvin, B.R., Martin, R.D., 2008. Endocranial volumes of primate species: scaling analyses using a comprehensive and reliable data set. J. Hum. Evol. 55, 967–978.

IUCN, 2014. IUCN Red List of Threatened Species. Version 2014.1. www.iucnredlist.org. Downloaded on 24 June 2014.

Kembel, S.W., Cowan, P.D., Helmus, M.R., Cornwell, W.K., Morlon, H., Ackerly, D.D., Blomberg, S.P., Webb, C.O., 2010. Picante: R tools for integrating phylogenies and ecology. Bioinformatics 26, 1463–1464.

Klingenberg, C.P., 2008. Morphological integration and developmental modularity. A. Rev. Ecol. Evol. Syst 39, 115–132.

Lieberman, D.E., Ross, C.F., Ravosa, M.J., 2000. The primate cranial base: ontogeny, function, and integration. Am. J. Phys. Anthropol 113 (s 31), 117–169.

Lieberman, D.E., Hallgrímsson, B., Liu, W., Parsons, T.E., Jamniczky, H.A., 2008. Spatial packing, cranial base angulation, and craniofacial shape variation in the mammalian skull: testing a new model using mice. J. Anat 212 (6), 720–735.

Lockwood, C.A., Kimbel, W.H., Lynch, J.M., 2004. Morphometrics and hominoid phylogeny: support for a chimpanzee–human clade and differentiation among great ape subspecies. Proc. Natl. Acad. Sci. USA 101 (13), 4356–4360.

Marroig, G., Cheverud, J.M., 2001. A comparison of phenotypic variation and covariation patterns and the role of phylogeny, ecology and ontogeny during cranial evolution of New World monkeys. Evolution 55, 2576–2600.

Marroig, G., Cheverud, J.M., 2005. Size as a line of least evolutionary resistance: diet and adaptive morphological radiation in new world monkeys. Evolution 59, 1128–1142.

Martins, E.P., Hansen, T.F., 1997. Phylogenies and the comparative method: a general approach to incorporating phylogenetic information into the analysis of interspecific data. Am. Nat 149, 646–667.

McArdle, B., Rodrigo, A.G., 1994. Estimating the ancestral states of a continuous-valued character using squared-change parsimony: an analytical solution. Syst. Biol 43, 573–578.

Mitteroecker, P., Gunz, P., 2009. Advances in geometric morphometrics. Evol. Biol. 36, 235–247.

Moen, D.S., Irschick, D.J., Wiens, J.J., 2013. Evolutionary conservatism and convergence both lead to striking similarity in ecology, morphology and performance across continents in frogs. Proc. R. Soc. B Biol. Sci. 280, 20132156.

Moss, M.L., 1972. Twenty years of functional cranial analysis. Am. J. Orthodont 61, 479–485.

Moss, M.L., Young, R.W., 1960. A functional approach to craniology. Am. J. Phys. Anthropol 18, 281–292.

Neaux, D., Guy, F., Gilissen, E., Coudyzer, W., Ducrocq, S., 2013. Covariation between midline cranial base, lateral basicranium, and face in modern humans and chimpanzees: a 3D geometric morphometric analysis. Anat. Rec 296, 568–579.

Neubauer, S., Gunz, P., Hublin, J.-J., 2009. The pattern of endocranial ontogenetic shape changes in humans. J. Anat 215, 240–255.

Opazo, J.C., Wildman, D.E., Prychitko, T., Johnson, R.M., Goodman, M., 2006. Phylogenetic relationships and divergence times among New World monkeys (Platyrrhini, Primates). Mol. Phylogenet. Evol 40, 274–280.

Orme, D., 2013. The caper package: comparative analysis of phylogenetics and evolution in R. R package version 0.5, 2.

Perelman, P., Johnson, W.E., Roos, C., Seuánez, H.N., Horvath, J.E., Moreira, M.A., Kessing, B., Pontius, J., Roelke, M., Rumpler, Y., Schneider, M.P.C., Silva, A., O'Brien, S.J., Pecon-Slattery, J., 2011. A molecular phylogeny of living primates. PLoS Genetics 7, e1001342.

Peres-Neto, P.R., Jackson, D.A., 2001. How well do multivariate data sets match? The advantages of a Procrustean superimposition approach over the Mantel test. Oecologia 129, 169–178.

Perez, S.I., Bernal, V., Gonzalez, P.N., 2006. Differences between sliding semi-landmark methods in geometric morphometrics, with an application to human craniofacial and dental variation. J. Anat 208, 769–784.

Perez, S.I., Klaczko, J., Rocatti, G., Dos Reis, S.F., 2011. Patterns of cranial shape diversification during the phylogenetic branching process of New World monkeys (Primates: Platyrrhini). J. Evol. Biol. 24, 1826–1835.

Perez, S.I., Klaczko, J., dos Reis, S.F., 2012. Species tree estimation for a deep phylogenetic divergence in the New World monkeys (Primates: Platyrrhini). Mol. Phylogenet. Evol. 65, 621–630.

Perez, S.I., Tejedor, M.F., Novo, N.M., Aristide, L., 2013. Divergence times and the evolutionary radiation of New World monkeys (Platyrrhini, Primates): an analysis of fossil and molecular data. Plos One 8, 68029.

Polly, P.D., 2003. Paleophylogeography: the tempo of geographic differentiation in marmots (Marmota). J. Mammal 84, 369–384.

R Core Team, 2014. R: A language and environment for statistical computing. R Foundation for Statistical Computing, Vienna, Austria. URL: http://www.R-project.org/.

Revell, L.J., 2012. phytools: an R package for phylogenetic comparative biology (and other things). Methods Ecol. Evol. 3, 217–223.

Revell, L.J., 2013. Two new graphical methods for mapping trait evolution on phylogenies. Methods Ecol. Evol. 4, 754–759.

Revell, L.J., Harmon, L.J., Collar, D.C., 2008. Phylogenetic signal, evolutionary process, and rate. Syst. Biol. 57, 591–601.

Rohlf, F.J., 2001. Comparative methods for the analysis of continuous variables: geometric interpretations. Evolution 55, 2143–2160.

Rohlf, F.J., Slice, D., 1990. Extensions of the Procrustes method for the optimal superimposition of landmarks. Syst. Biol. 39, 40–59.

Rosenberger, A.L., 1992. Evolution of feeding niches in New World monkeys. Am. J. Phys. Anthropol 88, 525–562.

Rosenberger, A.L., 2002. Platyrrhine paleontology and systematics: the paradigm shifts. In: Hartwig, W.C. (Ed.), The Primate Fossil Record. Cambridge University Press, Cambridge, pp. 151–160.
Rosenberger, A.L., Hartwig, W.C., 2001. New World Monkeys. Encyclopedia of Life Sciences. Nature Publishing Group.
Rosenberger, A.L., Tejedor, M.F., 2013. The misbegotten: long lineages, long branches and the interrelationships of *Aotus, Callicebus* and the saki-uakaris. In: Barnett, A.L., Veiga, S., Ferrari, S., Norconk, M.N. (Eds.), Evolutionary biology and conservation of Titis, Sakis and Uacaris. Cambridge University Press, Cambridge.
Rosenberger, A.L., Tejedor, M.F., Cooke, S.B., Pekar, S., 2009. Platyrrhine ecophylogenetics in space and time. In: Garber, P.A., Estrada, A., Bicca-Marques, J.C., Heymann, E.W., Strier, K.B. (Eds.), South American Primates. Springer, New York, pp. 69–113.
Ross, C.F., Henneberg, M., 1995. Basicranial flexion, relative brain size, and facial kyphosis in *Homo sapiens* and some fossil hominids. Am. J. Phys. Anthropol 98, 575–593.
Ross, C.F., Ravosa, M.J., 1993. Basicranial flexion, relative brain size, and facial kyphosis in nonhuman primates. Am. J. Phys. Anthropol 91, 305–324.
Rylands, A.B., Mittermeier, R.A., Silva, J.S., 2012. Neotropical primates: taxonomy and recently described species and subspecies. Int. Zool. Yrbk 46, 11–24.
Schluter, D., Price, T., Mooers, A.Ø., Ludwig, D., 1997. Likelihood of ancestor states in adaptive radiation. Evolution 51, 1699–1711.
Smith, R.J., Jungers, W.L., 1997. Body mass in comparative primatology. J. Hum. Evol. 32, 523–559.
Sperber, G.H., 2001. Craniofacial development. BC Decker Inc., Hamilton.
Wiens, J.J., Ackerly, D.D., Allen, A.P., Anacker, B.L., Buckley, L.B., Cornell, H.V., Damschen, E.I., Jonathan Davies, T., Grytnes, J.-A., Harrison, S.P., Hawkins, B.A., Holt, R.D., McCain, C.M., Stephens, P.R., 2010. Niche conservatism as an emerging principle in ecology and conservation biology. Ecology Letters 13, 1310–1324. http://dx.doi.org/10.1111/j.1461-0248.2010.01515.x.
Wildman, D.E., Jameson, N.M., Opazo, J.C., Yi, S.V., 2009. A fully resolved genus level phylogeny of neotropical primates (Platyrrhini). Mol. Phylogenet. Evol. 53, 694–702.
Wiley, D.F., Amenta, N., Alcantara, D.A., Ghosh, D., Kil, Y.J., Delson, E., Harcourt-Smith, W., Rohlf, F.J., St. John, K., Hamann, B., Motani, R., Frost, S., Rosenberger, A.L., Tallman, L., Disotell, T., O'Neill, R., 2005. Evolutionary morphing. In: Visualization, 2005. VIS 05, IEEE, pp. 431–438.
van Woerden, J.T., Schaik, C.P., Isler, K., 2014. Seasonality of diet composition is related to brain size in New World Monkeys. Am. J. Phys. Anthropol 154, 628–632.
Yushkevich, P.A., Piven, J., Hazlett, H.C., Smith, R.G., Ho, S., Gee, J.C., Gerig, G., 2006. User-guided 3D active contour segmentation of anatomical structures: significantly improved efficiency and reliability. Neuroimage 31, 1116–1128.